

High-precision Q -value measurement and nuclear matrix elements for the double- β decay of ^{98}Mo

D.A. Nesterenko^{a,*}, L. Jokiniemi^b, J. Kotila^{a,c}, A. Kankainen^a, Z. Ge^a, T. Eronen^a, S. Rinta-Antila^a, J. Suhonen^a

^aUniversity of Jyväskylä, P.O. Box 35, FI-40014 University of Jyväskylä, Finland

^bDepartment of Quantum Physics and Astrophysics and Institute of Cosmos Sciences, University of Barcelona, 08028 Barcelona, Spain

^cCenter for Theoretical Physics, Sloane Physics Laboratory, Yale University, New Haven, Connecticut 06520-8120, USA

Abstract

Neutrinoless double-beta ($0\nu\beta\beta$) decay and the standard two-neutrino double-beta ($2\nu\beta\beta$) decay of ^{98}Mo have been studied. The double-beta decay Q -value has been determined as $Q_{\beta\beta} = 113.668(68)$ keV using the JYFLTRAP Penning trap mass spectrometer. It is in agreement with the literature value, $Q_{\beta\beta} = 109(6)$ keV, but almost 90 times more precise. Based on the measured Q -value, precise phase-space factors for $2\nu\beta\beta$ decay and $0\nu\beta\beta$ decay, needed in the half-life predictions, have been calculated. Furthermore, the involved nuclear matrix elements have been computed in the proton-neutron quasiparticle random-phase approximation (pnQRPA) and the microscopic interacting boson model (IBM-2) frameworks. Finally, predictions for the $2\nu\beta\beta$ decay are given, suggesting a much longer half-life than for the currently observed cases.

Keywords: Double- β decay, Binding energies and masses, Mass spectrometers, Penning trap, Nuclear matrix elements, Phase-space factors

1. Introduction

Double-beta ($\beta\beta$) decay is a nuclear process in which two neutrons turn into protons (or vice versa) and two electrons are emitted. In the standard, two-neutrino double-beta ($2\nu\beta\beta$) decay, the emitted electrons are accompanied by two antineutrinos and hence the lepton number is conserved. Such process has already been observed in about a dozen nuclei, where β decay is energetically forbidden or very suppressed [1]. However, there is also a hypothetical version of $\beta\beta$ decay, namely neutrinoless double-beta ($0\nu\beta\beta$) decay, where only two electrons are emitted. This process violates the lepton-number conservation law of the standard model (SM) of particle physics by two units, since two leptons are created. The process would only be possible if neutrino is a Majorana particle (meaning its own antiparticle) first hypothesized by Ettore Majorana in 1937 [2]. The observation of $0\nu\beta\beta$ decay would therefore answer the open questions about beyond-SM physics such as the matter-antimatter symmetry of the Universe [3, 4] and the nature of neutrinos [5, 6, 7, 8, 9].

The neutrinoless mode is under massive searches by several large-scale experiments worldwide [10, 11, 12, 13, 14, 15, 16], with the most stringent half-life limits given by $t_{1/2}^{0\nu} \gtrsim 10^{26}$ y, while the measured half-lives of $2\nu\beta\beta$ decay are of the order $t_{1/2}^{2\nu} \sim 10^{18} - 10^{24}$ y [1]. Another intriguing aspect of $0\nu\beta\beta$ decay is that the half-life of the

process is inversely proportional to the square of the effective Majorana mass that depends on the neutrino masses. Hence, one could obtain estimates for the neutrino masses (at present, only the differences of the squares are known) from the measured half-lives [17, 18]. The next-generation $\beta\beta$ -decay experiments are aiming to fully cover the inverted-hierarchy (meaning that the neutrino mass states follow the ordering $m_3 < m_1 \lesssim m_2$) region of the neutrino masses [19]. However, in order to interpret the results, one needs reliable phase-space factors and $\beta\beta$ -decay nuclear matrix elements (NMEs), which need to be predicted from nuclear theory. While the phase-space factors can be accurately calculated [20], the present predictions for the $0\nu\beta\beta$ -decay NMEs from different theory frameworks disagree by more than a factor of two [7].

In the present paper, we study one of the possible $\beta\beta$ emitters, ^{98}Mo . So far, there has been no direct Q -value measurement for the double-beta decay transition between the nuclear ground states $^{98}\text{Mo} \rightarrow ^{98}\text{Ru}$. The literature Q -value, 109(6) keV [21], has been limited by the uncertainty in the mass value of ^{98}Ru . It is mainly based on the mass difference between C_7H_{14} and ^{98}Ru measured using a sixteen-inch double-focusing mass spectrometer in 1960s [22]. In this work, we determine the Q value by a direct frequency-ratio measurement of singly-charged $^{98}\text{Mo}^+$ and $^{98}\text{Ru}^+$ ions in the JYFLTRAP Penning trap [23]. In addition, we have measured the Q -value for the double-electron capture of ^{96}Ru and compared it to the high-precision measurement ($\delta m/m \approx 1.4 \times 10^{-9}$) done at the SHIPTRAP Penning trap [24].

*Corresponding author

Email address: dmitrii.nesterenko@jyu.fi (D.A. Nesterenko)

Based on the measured Q -value for the $\beta\beta$ -decay of ^{98}Mo , we calculate the phase-space factors for the two-neutrino and the neutrinoless decay modes. Furthermore, we calculate the NMEs for the two decay modes in two different theory frameworks that are well established for calculating the NMEs in medium-heavy to heavy nuclei: proton-neutron quasiparticle random-phase approximation (pnQRPA) [25, 26] and microscopic interacting boson model (IBM-2) [27, 28]. This is the first time the ^{98}Mo double-beta decay matrix elements are calculated in no-core pnQRPA and IBM-2 frameworks. Due to the low Q -value, the $2\nu\beta\beta$ -decay has not been measured - hence, we give estimates for both the $2\nu\beta\beta$ -decay and $0\nu\beta\beta$ -decay half-lives based on the calculated NMEs and phase-space factors.

2. Double-beta decay

2.1. Two-neutrino double-beta decay

The $2\nu\beta\beta$ -decay half-life can be written in the form

$$[t_{1/2}^{2\nu}]^{-1} = G_{2\nu} (g_A^{\text{eff}})^4 |M^{2\nu}|^2, \quad (1)$$

where $G_{2\nu}$ is a phase-space factor for the final-state leptons [20] for the two-neutrino mode and $M^{2\nu}$ is the $2\nu\beta\beta$ -decay NME. Here g_A^{eff} is the effective value of the axial-vector coupling, quenched relative to the free-nucleon value $g_A \simeq 1.27$, as found in many different nuclear-structure calculations for the medium-mass and heavy nuclei along the years (see the recent reviews [9, 29]). The NME can be written as

$$M^{2\nu} = M_{\text{GT}}^{2\nu} + \left(\frac{g_V}{g_A}\right)^2 M_{\text{F}}^{2\nu}, \quad (2)$$

with Gamow-Teller (GT) and Fermi (F) parts and the vector coupling $g_V = 1.0$ [25]. In the case of $2\nu\beta\beta$ decay, if isospin is a good quantum number, the Fermi matrix elements should identically vanish. Thus, in both pnQRPA and IBM-2 calculations the Fermi part of the matrix element is forced to be zero in order to restore isospin symmetry, as explained in Section 4.2.

2.2. Neutrinoless double-beta decay

The $0\nu\beta\beta$ -decay half-life can be written as [7]

$$[t_{1/2}^{0\nu}]^{-1} = G_{0\nu} (g_A^{\text{eff}})^4 |M^{0\nu}|^2 \frac{m_{\beta\beta}^2}{m_e^2}, \quad (3)$$

where $G_{0\nu}$ is a phase-space factor for the final-state leptons [20] in the neutrinoless mode, and $M^{0\nu}$ is the light-neutrino-exchange $0\nu\beta\beta$ -decay NME. The effective Majorana mass $m_{\beta\beta} = \sum_i U_{ei} m_i$ (normalized to the electron mass m_e) characterizes the lepton-number violation and depends on the neutrino masses m_i and mixing matrix U .

The matrix element $M^{0\nu}$ in Eq. (3) consists of Gamow-Teller (GT), Fermi (F) and tensor (T) parts and can be written as [7]

$$M^{0\nu} = M_{\text{GT}}^{0\nu} - \left(\frac{g_V}{g_A}\right)^2 M_{\text{F}}^{0\nu} + M_{\text{T}}^{0\nu}. \quad (4)$$

3. Experimental method and results

The Q -value measurements have been performed using the JYFLTRAP Penning trap mass spectrometer [23] at the Ion Guide Isotope Separator On-Line (IGISOL) facility [30]. The ions of interest were separately produced using two electric discharge ion sources, one with natural ruthenium in the IGISOL target chamber [31] and the other with natural molybdenum at the offline ion source station [32]. Most of the ions were produced as singly-charged and accelerated to 30 keV. An electrostatic deflector selected ions from one ion source at a time, blocking the ions from the other source. The ions were mass-separated using a 55° dipole magnet and the continuous beam with the selected mass number A was injected into a gas-filled radiofrequency quadrupole (RFQ) [33]. The cooled and bunched ion beam after the RFQ was transported to the JYFLTRAP Penning traps placed inside a 7-T superconducting magnet.

In the first (preparation) trap the ions were cooled, centered and additionally purified using a mass-selective buffer gas cooling technique [34]. In the second (measurement) trap the cyclotron frequency for an ion with mass m and charge q in the magnetic field B , given by

$$\nu_c = \frac{1}{2\pi} \frac{q}{m} B, \quad (5)$$

was measured employing the phase-imaging ion-cyclotron-resonance (PI-ICR) technique [35, 36, 37].

The ion's cyclotron frequency ν_c was determined as a sum of its radial-motion frequencies in the trap, a magnetron frequency ν_- and a modified cyclotron frequency ν_+ . The measurements followed the scheme described in Ref. [36]. Two excitation patterns were applied alternately in order to determine the accumulated magnetron and cyclotron phases of the ion motion. After injecting the ions into the measurement trap, the coherent component of the magnetron motion was reduced by applying 600- μs dipolar radiofrequency (rf) pulse at the magnetron frequency ν_- . Then, the cyclotron motion of the ions was excited to an amplitude of about 1 mm through application of a 100- μs dipolar rf pulse at the modified cyclotron frequency ν_+ . After the excitation, the ion's cyclotron motion was converted into the magnetron motion via a 2-ms quadrupolar rf pulse at the frequency close to the cyclotron frequency ν_c . The ions accumulated the magnetron-motion phase during the phase accumulation time t_{acc} of free rotation and were then extracted from the trap. For the measurement of the cyclotron-motion phase the ions accumulated the cyclotron phase after ν_+ -pulse for the phase accumulation time t_{acc} , which was followed by a conversion pulse applied before the extraction from the trap. The radial motion phase of the ions extracted from the trap was projected onto a position-sensitive detector (microchannel plate detector with a delay line anode).

The positions of the magnetron and cyclotron phase images on the detector, defined by the polar angles α_-

Table 1: The weighted means (\bar{R}) of the measured frequency ratios $R = \nu_c(\text{daughter})/\nu_c(\text{parent})$ and the corresponding Q -values for the studied transitions. The literature Q -values and differences to the literature values are also given.

Transition	Frequency ratio \bar{R}	Q -value (keV)	Lit. Q -value (keV)	Difference (keV)
$^{98}\text{Mo} \rightarrow ^{98}\text{Ru}$	1.000 001 246 39(74)	113.668(68)	109(6) [21]	4.7(60)
$^{96}\text{Ru} \rightarrow ^{96}\text{Mo}$	1.000 030 386 86(55)	2714.583(50)	2714.51(13) [24]	0.073(139)

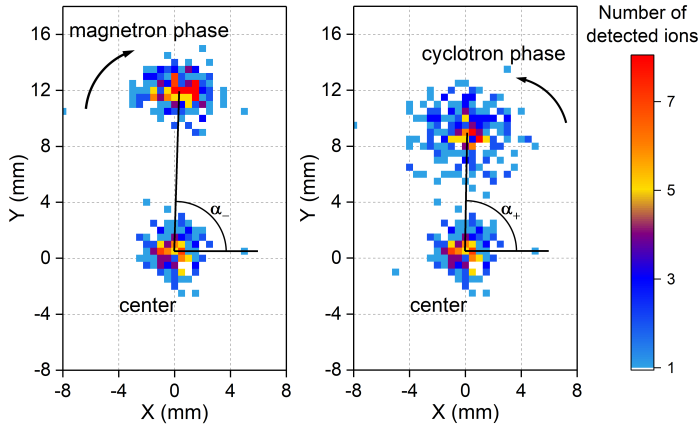


Figure 1: Projection of the trap center and accumulated phase spots for $^{98}\text{Mo}^+$ ions on the position-sensitive MCP detector in a single 4.5-min cyclotron frequency measurement with the PI-ICR method. The phase accumulation time t_{acc} was about of 500 ms.

and α_+ , correspondingly, with respect to the trap center, were chosen such that the angle $\alpha_c = \alpha_+ - \alpha_-$ did not exceed a few degrees. It is required to minimize the systematic shifts due to the distortion of the projection on the detector and reduce the influence from the conversion of the cyclotron motion to the magnetron motion [36]. The cyclotron frequency is determined from the angle between two phase images as:

$$\nu_c = \nu_- + \nu_+ = \frac{\alpha_c + 2\pi n}{2\pi t_{acc}}, \quad (6)$$

where n is the full number of revolutions, which the studied ions would perform in a magnetic field B in absence of electric field during a phase accumulation time t_{acc} .

The phase spots and the center spot were alternately accumulated during a single 4.5-min cyclotron frequency measurement (see Fig. 1). About 300 ions were collected for each spot. Any residual magnetron and cyclotron motion could lead to shifts of the phase position. To eliminate these effects, the start time of the cyclotron excitation was repeatedly scanned over a magnetron period ($\approx 600 \mu\text{s}$) and the start time of the extraction pulse was scanned over a cyclotron period ($\approx 0.9 \mu\text{s}$).

The cyclotron frequencies of the parent nuclide ν_c^p and the daughter nuclide ν_c^d were alternately measured changing every 4.5 minutes. The frequency ν_c^d measured before and after the ν_c^p measurement, was linearly interpolated to the time of the ν_c^p measurement and a single cyclotron frequency ratio $R_i = \nu_c^d/\nu_c^p$ was determined. The systematic uncertainty due to non-linear changes of the magnetic

field was negligible compared to the achieved statistical uncertainty [38]. The final cyclotron frequency ratio \bar{R} was calculated as a weighted mean of R_i . The ions of the parent and daughter nuclides were measured in similar conditions to minimize a possible systematic shift of the frequency ratio due to imperfections of the measurement trap. Mass-dependent systematic effects are negligible compared to the statistical uncertainty for mass doublets [39]. Count-rate class analysis [40, 39] was performed and no correlations between the frequency ratios and the number of detected ions per bunch were observed. Up to 5 ions/bunch were taken into account in the analysis.

The Q -value is calculated from the cyclotron frequency ratio as

$$Q = (M_p - M_d)c^2 = \left(\frac{\nu_c^d}{\nu_c^p} - 1\right)(M_d - m_e)c^2, \quad (7)$$

where M_p and M_d are the atomic masses and ν_c^p and ν_c^d the cyclotron frequencies of the parent and daughter nuclides, correspondingly, m_e is the electron mass and c is the speed of light in vacuum. The difference in binding energies of valence electron in Mo and Ru is less than 1 eV [41], and has been neglected. The atomic mass unit used in the analysis is $u = 931494.10242(28) \text{ keV}/c^2$ [42].

The cyclotron frequency ratios $R_i = \nu_c(^{98}\text{Ru}^+)/\nu_c(^{98}\text{Mo}^+)$, measured at JYFLTRAP, are shown in Fig. 2. The phase accumulation time t_{acc} of about 500 ms was chosen to ensure that the cyclotron spot was not overlapping with any possible isobaric contamination on the detector. The final weighted mean frequency ratio is $\bar{R} = 1.00000124639(74)$ resulting in a $Q_{\beta\beta}$ -value of 113.668(68) keV. Using the determined $Q_{\beta\beta}$ -value of ^{98}Mo and the mass-excess value of ^{98}Mo from AME20, -88115.98(17) keV [21], we also improve the mass-excess value for ^{98}Ru considerably, from -88225(6) keV in AME20 [21] to -88229.65(19) keV.

Similarly, the Q -value of double-electron capture in ^{96}Ru was measured using the PI-ICR technique with the phase accumulation time t_{acc} of about 510 ms. The results are given in Table 1. The measured $Q_{\epsilon\epsilon}$ -value of ^{96}Ru , 2714.583(50) keV, is in a good agreement with the SHIP-TRAP $Q_{\epsilon\epsilon}$ -value, 2714.51(13) keV [24], and 2.6 times more precise. This measurement provides an additional cross-check of our accuracy with Mo and Ru ions in the studied mass region.

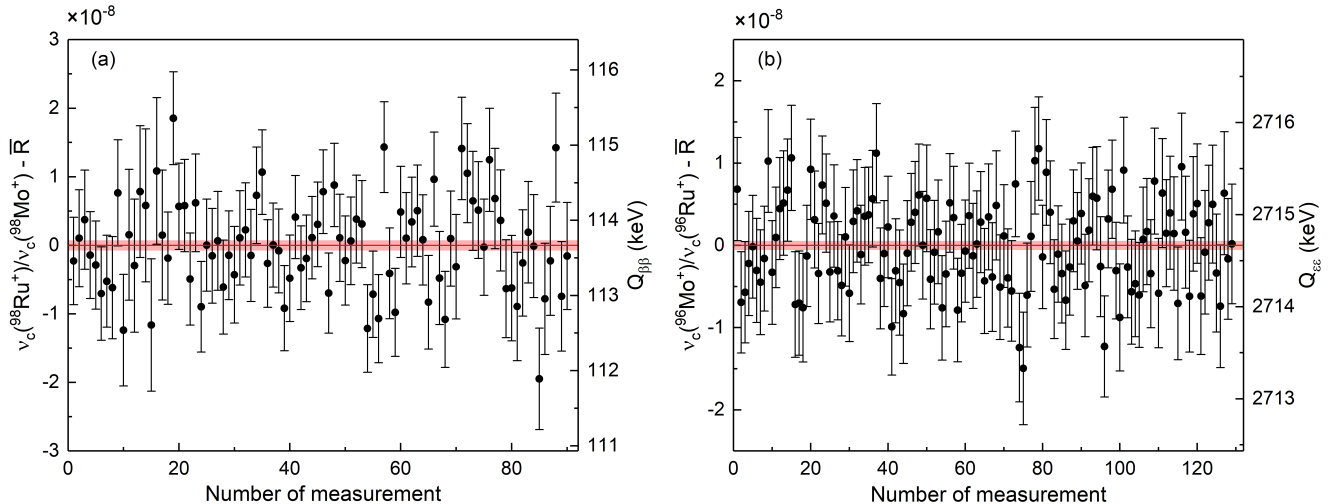


Figure 2: Cyclotron frequency ratios (a) $\bar{R} = \nu_c(^{98}\text{Ru}^+)/\nu_c(^{98}\text{Mo}^+)$ and (b) $\bar{R} = \nu_c(^{96}\text{Mo}^+)/\nu_c(^{96}\text{Ru}^+)$ measured in this work. The red band represents the total 1σ uncertainty of the weighted mean frequency ratio \bar{R} . For \bar{R} see Table 1.

4. Theory predictions

4.1. Phase-space factors

The key ingredient for the evaluation of phase-space factors (PSF) in single- and double- β decay are the electron wave functions. These energy-dependent wave functions are used to form decay-mechanism specific combinations and then integrated over available electron energies up to the end-point energy dictated by the Q -value. A general theory of phase-space factors in $\beta\beta$ -decay was developed years ago by Doi *et al.* [43, 44] following the previous work of Primakoff and Rosen [45]. It was reformulated by Tomoda [46] who also presented results for selected nuclei. However, in these earlier calculations approximate expression for the electron wave functions at the nucleus was used. Here we evaluate the PSFs using exact Dirac electron wave functions and including screening by the electron cloud by following the procedure given in Ref. [20]. The obtained PSFs for ^{98}Mo are: $G_{0\nu} = 6.18 \times 10^{-18}\text{y}^{-1}$ and $G_{2\nu} = 3.71 \times 10^{-29}\text{y}^{-1}$ for the neutrinoless and two-neutrino double-beta decay, respectively.

4.2. Nuclear matrix elements

The pnQRPA calculations in the present study are based on the spherical version of pnQRPA with large no-core single-particle bases, similarly as in Refs. [47, 48]. The single-particle bases consist of 25 orbitals - from the lowest $0s_{1/2}$ orbit up to the $0i_{13/2}$ orbit. We take the single-particle energies from a Coulomb-corrected Woods-Saxon potential [49]. The quasiparticle spectra, needed in the pnQRPA diagonalization, are obtained by solving the BCS equations using a pairing interaction based on the Bonn-A meson-exchange potential [50] for protons and neutrons separately. The interaction is fine-tuned by adjusting the pairing parameters to reproduce the phenomenological pairing gaps. The residual Hamiltonian of the pnQRPA calculation contains two adjustable parameters: the

particle-particle g_{pp} and the particle-hole g_{ph} parameters [51]. The particle-hole parameter is adjusted to reproduce the location of the Gamow-Teller giant resonance in ^{98}Tc . It is a well-known feature [51] that the β - and $\beta\beta$ -decay NMEs are sensitive to the value of particle-particle parameter g_{pp} , as demonstrated in the present calculations in Fig. 3. Here we follow the so-called partial isospin restoration scheme [52], and divide the parameter into isoscalar ($T = 0$) and isovector ($T = 1$) parts which multiply the isoscalar and isovector channels of the calculations, respectively. The strength $g_{pp}^{T=1}$ of the isovector channel is then adjusted so that the Fermi part of the $2\nu\beta\beta$ -decay NME vanishes. Ideally, the isoscalar strength $g_{pp}^{T=0}$ would then be fixed so that $M_{GT}^{2\nu}$ reproduces the measured $2\nu\beta\beta$ -decay half-life, but since it has not been measured for ^{98}Mo , we adjust $g_{pp}^{T=0}$ to the observed Gamow-Teller transition $^{98}\text{Nb}(1_{g.s}^+) \rightarrow ^{98}\text{Mo}(0_{g.s}^+)$ with $\log ft = 4.72$, instead.

Since the Fermi part of the $2\nu\beta\beta$ NMEs is forced to zero, the $2\nu\beta\beta$ decay runs only through the 1^+ virtual states of the intermediate nucleus. Hence, the $2\nu\beta\beta$ -decay NME is calculated by summing over the 1^+ states. On the other hand, $0\nu\beta\beta$ decays run through all J_i^π states in the intermediate nucleus. In the pnQRPA framework, the $0\nu\beta\beta$ -decay NMEs are calculated without resorting to the so-called closure approximation by explicitly summing over the intermediate states (see e.g. [25, 26]). The wave functions and excitation energies of the states in an odd-odd nucleus are obtained from a pnQRPA diagonalization based on a neighboring even-even reference nucleus [53]. Here, due to the involved two steps of the $\beta\beta$ decay, they are computed in the intermediate odd-odd nucleus ^{98}Tc by starting from the ^{98}Mo and ^{98}Ru reference nuclei. Hence, we obtain two sets of the intermediate states, which is taken into account as an overlap factor in the NMEs [25, 51].

Another frequently used model to evaluate $\beta\beta$ NMEs is the microscopic interacting boson model (IBM-2) [54, 55].

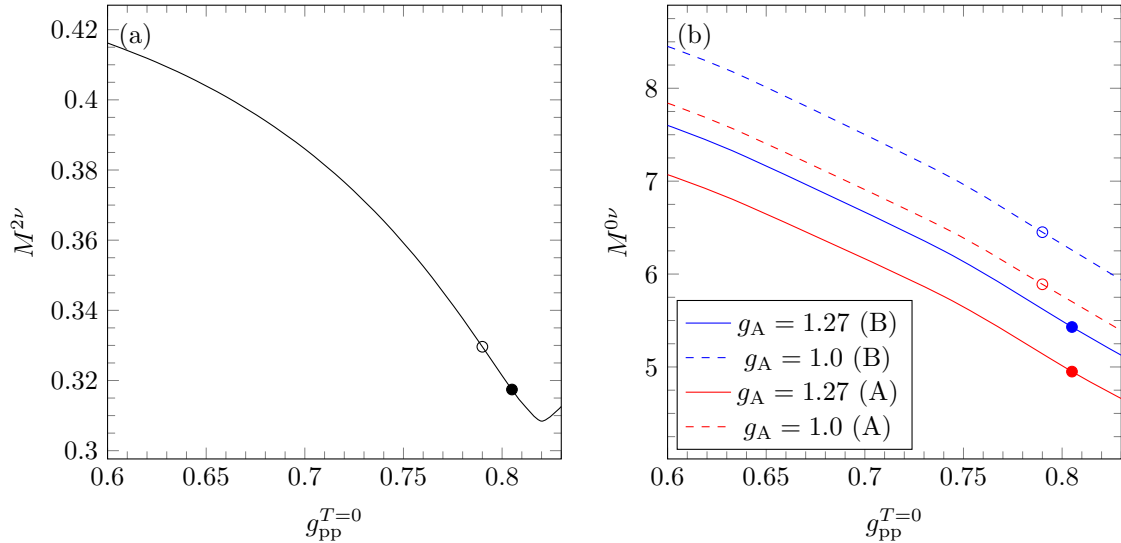


Figure 3: The (a) $2\nu\beta\beta$ -decay and (b) $0\nu\beta\beta$ -decay NMEs of the transition $^{98}\text{Mo}(0_{g.s.}^+) \rightarrow ^{98}\text{Ru}(0_{g.s.}^+)$ as functions of the particle-particle parameter $g_{pp}^{T=0}$ in the pnQRPA framework. The solid (open) circles correspond to the $g_{pp}^{T=0}$ adjusted to the $\log ft$ -value of the transition $^{98}\text{Nb}(1_{g.s.}^+) \rightarrow ^{98}\text{Mo}(0_{g.s.}^+)$ with $g_A^{\text{eff}} = 1.27$ ($g_A^{\text{eff}} = 1.0$). 'A' refers to the Argonne and 'B' to the CD-Bonn SRC-parametrization.

The method of evaluation is discussed in detail in [27, 28]. The logic of the method is to map [56] the fermion Hamiltonian H onto a boson space and evaluate it with bosonic wave functions. The single-particle and -hole energies and strengths of interaction were evaluated and discussed in detail in Ref. [57] where the occupancies of the single-particle levels were calculated in order to satisfy a twofold goal: to assess the goodness of the single-particle energies and to check the reliability of the used wave functions. Both tests are particularly important in the case of nuclei involved in double beta decay, as they affect the evaluation of the NMEs and thus their reliability [58].

In IBM-2 the isospin is restored by modifying the mapped operator by imposing the condition that $M_F^{(2\nu)} = 0$. This condition is simply implemented in the calculation by replacing the radial integrals of Appendix A of Ref. [27] with ones given in Eqs. (9) and (10) in [28] that guarantee that the Fermi matrix elements vanish for $2\nu\beta\beta$ decay, as discussed in [28]. This replacement also reduces the Fermi matrix elements for $0\nu\beta\beta$ decay by quenching the monopole term from the multipole expansion of the matrix element. Even though the method of isospin restoration is similar in spirit to that of pnQRPA, it is different in practise.

In the IBM-2 calculations closure approximation is assumed. The main idea behind the closure approximation is to replace the energies of the intermediate states with an average energy, and then the sum over the intermediate states can be removed by using the completeness relation. In [59] the sensitivity of the $0\nu\beta\beta$ NME to the closure energy ($\sim 10\text{MeV}$) is estimated to be only 5 %, owing to the fact that the momentum of the virtual neutrino is of the order of 100 – 200 MeV, i.e., much larger than the typical nuclear excitations.

Since the effective value of the axial coupling g_A in finite nuclei is under debate [29, 60, 61], we calculate the $2\nu\beta\beta$ - and $0\nu\beta\beta$ -decay NMEs with two different effective g_A values: the free-nucleon value 1.27 and a standard "shell-model-type" quenched value 1.0. As can be seen from Eq. (2), the $2\nu\beta\beta$ -decay NME, once the Fermi part is forced to zero, does not depend on g_A . However, the g_A -dependence of the NME in the pnQRPA framework stems from the way we adjust the parameter g_{pp} , in the present case using the decay rate of a β -decay transition. The many-body states involved in the $0\nu\beta\beta$ -decay NMEs are corrected for the two-nucleon short-range correlations (SRCs) following the so-called CD-Bonn and Argonne parametrizations [62]. The resulting NMEs for $2\nu\beta\beta$ and $0\nu\beta\beta$ decays are shown in Tables 2 and 3, respectively. For $2\nu\beta\beta$ decay we also show the half-lives obtained from Eq. (1) with the calculated phase-space factors and NMEs. For comparison, we show the half-lives obtained in projected Hartree-Fock-Bogoliubov (PHFB) [63] and in the self-consistent renormalized QRPA (SRQRPA) [64] frameworks with less precise estimates for the phase-space factor. As for $0\nu\beta\beta$ -decay, it is hard to give estimates for the half-life, since it depends on the unknown Majorana mass (see Eq. (3)). Hence, in Table 4 we give estimates for the half-life for a Majorana mass range of $0.01 \text{ eV} < m_{\beta\beta} < 0.1 \text{ eV}$, which covers the part of the inverted-hierarchy band of Majorana mass allowed by cosmological searches – the region the next-generation experiments are interested in.

As can be seen from Table 2, the predicted half-lives of the $2\nu\beta\beta$ -decay are of the order of $t_{1/2}^{2\nu} \sim 10^{29} \text{ y}$ – much longer than the currently observed half-lives in other nuclei, owing to the low Q -value $\sim 100 \text{ keV}$ of the presently discussed transition. For the measured decays the Q -values

Table 2: The $2\nu\beta\beta$ -decay NMEs and the resulting half-lives with different effective g_A values for the transition $^{98}\text{Mo} \rightarrow ^{98}\text{Ru}$ calculated in the pnQRPA and IBM-2 frameworks. The half-life results are compared with available other calculations.

g_A^{eff}	$M^{2\nu}$		$t_{1/2}^{2\nu} (10^{29} \text{ y})$			
	pnQRPA	IBM-2	pnQRPA	IBM-2	PHFB [63]	SRQRPA [64]
1.27	0.317	0.380	1.031	0.718	6.09	4.06 – 15.2
1.0	0.330	0.380	2.475	1.867	14.87	

Table 3: The $0\nu\beta\beta$ -decay NMEs for the transition $^{98}\text{Mo} \rightarrow ^{98}\text{Ru}$ calculated in the pnQRPA and IBM-2 frameworks with different short-range correlations (SRC) and values of g_A^{eff} . Here $M'^{0\nu}$ refers to the so-called "effective" NME $(g_A^{\text{eff}}/g_A)^2 M^{0\nu}(g_A^{\text{eff}})$.

SRC	g_A^{eff}	pnQRPA					IBM-2				
		$M_F^{0\nu}$	$M_{GT}^{0\nu}$	$M_T^{0\nu}$	$M^{0\nu}$	$M'^{0\nu}$	$M_F^{0\nu}$	$M_{GT}^{0\nu}$	$M_T^{0\nu}$	$M^{0\nu}$	$M'^{0\nu}$
Argonne	1.27	-1.57	4.36	-0.38	4.95	4.95	-0.48	4.54	-0.26	4.58	4.58
Argonne	1.0	-1.58	4.72	-0.41	5.89	3.65	-0.48	4.62	-0.27	4.82	2.99
CD-Bonn	1.27	-1.69	4.76	-0.38	5.43	5.43	-0.52	4.70	-0.26	4.76	4.76
CD-Bonn	1.0	-1.69	5.17	-0.41	6.45	4.00	-0.52	4.78	-0.27	5.04	3.12

Table 4: The $0\nu\beta\beta$ -decay half-lives with different effective g_A values for the transition $^{98}\text{Mo} \rightarrow ^{98}\text{Ru}$ calculated in the pnQRPA and IBM-2 frameworks. The ranges correspond to the adopted range of Majorana mass, $0.01 \text{ eV} < m_{\beta\beta} < 0.1 \text{ eV}$.

g_A^{eff}	$t_{1/2}^{0\nu} (10^{29} \text{ y})$	
	pnQRPA	IBM-2
1.27	0.55 - 66.3	0.72 - 77.4
1.0	1.02 - 122	1.66 - 182

are of the order of ~ 1 MeV. The half-lives obtained in the present work are consistently smaller by a factor of $\approx 4 - 20$ than those obtained in the PHFB and SRQRPA frameworks, mostly due to the larger NMEs obtained in the present work. Contrary to this, the differences between the pnQRPA and IBM-2 predictions are notably smaller, IBM-2 giving some 15 – 20 % larger NMEs than pnQRPA.

As for $0\nu\beta\beta$ decay, one can see from Table 3 that the pnQRPA-computed effective NMEs $M'^{0\nu}$, obtained with $g_A^{\text{eff}} = 1.27$, are consistently larger by some 10 – 15% than the IBM-2-computed ones. With $g_A^{\text{eff}} = 1.0$ the difference is larger, 20 – 30 %, owing to the g_{pp} -adjustment method of pnQRPA, which partially compensates the quenching effect. The differences between the two calculations stem from the quite different magnitudes of the Fermi NME, which is some 3 times larger in the pnQRPA formalism than in the IBM-2, owing to the quenching of the monopole term from the multipole expansion of the IBM-2 Fermi NME. The pnQRPA- and IBM-2 -computed values of the Gamow-Teller NMEs are, however, quite close to each other. Interestingly, the NMEs obtained within both frameworks are smaller than the NMEs obtained in the PHFB framework [65], $M'^{0\nu}(g_A^{\text{eff}} = 1.254) = 5.94 - 7.13$ and $M'^{0\nu}(g_A^{\text{eff}} = 1.0) = 4.23 - 5.13$.

The $0\nu\beta\beta$ -decay half-life predictions in Table 4, ob-

tained from Eq. (3) with the NMEs of Table 3 and the Majorana mass range $0.01 \text{ eV} < m_{\beta\beta} < 0.1 \text{ eV}$, are ranging between $0.55 \times 10^{29} \text{ y}$ and $1.82 \times 10^{31} \text{ y}$. The smaller IBM-2 NMEs are reflected as slightly longer half-lives, but the ranges obtained in both frameworks are wide due to the uncertainty on the Majorana mass. The lower limits are similar to our half-life predictions for the $2\nu\beta\beta$ decay, but the upper limits are ~ 100 times larger. In any case, the half-lives are well beyond the half-life sensitivities of the current experiments $S_{1/2} \approx 10^{25} - 10^{26} \text{ y}$ (for other nuclei).

5. Discussion

We have determined the Q -value for the double-beta decay of ^{98}Mo directly for the first time using Penning-trap mass spectrometry. The obtained $Q_{\beta\beta} = 113.668(68)$ keV agrees with the $Q_{\beta\beta}$ -value given in AME2020, 109(6) keV [21], but is almost 90 times more precise. Based on the measured Q -value, the phase-space factors for the two-neutrino and neutrinoless double-beta-decay modes were computed. Furthermore, the nuclear matrix elements, involved in the half-life expressions of these decay modes, were calculated in the pnQRPA and IBM-2 frameworks. Within both frameworks we take the isospin restoration into account by forcing the Fermi matrix element of the $2\nu\beta\beta$ decay to vanish.

The presently obtained $2\nu\beta\beta$ half-lives are consistently smaller than those previously obtained in the PHFB [65] or in the SQRPA [64] framework, mostly due to larger NMEs obtained in pnQRPA and IBM-2. On the other hand, the differences between the pnQRPA and IBM-2 values are relatively small, IBM-2 giving some 15 – 20 % larger NMEs than pnQRPA. As for $0\nu\beta\beta$ decay, the NMEs obtained in pnQRPA and IBM-2 are consistently smaller than those obtained in the PHFB framework [65], but pn-

QRPA predicts some 10 – 30 % larger NMEs, depending on the value of g_A^{eff} and the SRC-parametrization. This difference largely pertains to the marked differences in the Fermi NME, the Gamow-Teller NMEs being roughly equal. All in all, the predictions given by the two models are in satisfactory agreement, bearing in mind that the theoretical foundations of the two approaches are quite different: The IBM-2 using the closure approximation and a quite restricted single-particle space with renormalized transition operators, and the pnQRPA including explicitly the intermediate virtual states and using a large no-core single-particle space with bare transition operators. According to both models, the half-life of the $2\nu\beta\beta$ -decay of ^{98}Mo , corresponding to the presently obtained Q -value, would be notably larger than the currently known experimental half-lives of some other double-beta nuclei.

Acknowledgements

This work has been supported by the Finnish Cultural Foundation (Grant No. 00210067) and the Academy of Finland (Grant Nos. 314733, 320062, 318043, 295207 and 327629). The funding from the European Union’s Horizon 2020 research and innovation programme under grant agreement No. 771036 (ERC CoG MAIDEN) is gratefully acknowledged.

References

- [1] A. Barabash, Precise half-life values for two-neutrino double- β decay: 2020 review, *Universe* 6 (2020) 159. doi:10.3390/universe6100159.
- [2] E. Majorana, Sulla simmetria tra particelle e antiparticelle [in italian], *Nuovo Cimento* 14 (1937) 322.
- [3] M. Fukugita, T. Yanagida, Baryogenesis Without Grand Unification, *Phys. Lett. B* 174 (1986) 45. doi:10.1016/0370-2693(86)91126-3.
- [4] S. Davidson, E. Nardi, Y. Nir, Leptogenesis, *Phys. Rept.* 466 (2008) 105. doi:10.1016/j.physrep.2008.06.002.
- [5] F. T. Avignone III, S. R. Elliott, J. Engel, Double beta decay, Majorana neutrinos, and neutrino mass, *Rev. Mod. Phys.* 80 (2008) 481. doi:10.1103/RevModPhys.80.481.
- [6] J. D. Vergados, H. Ejiri, F. Šimkovic, Theory of neutrinoless double-beta decay, *Rep. Prog. Phys.* 75 (2012) 106301. doi:10.1088/0034-4885/75/10/106301.
- [7] J. Engel, J. Menéndez, Status and future of nuclear matrix elements for neutrinoless double-beta decay: a review, *Rep. Prog. Phys.* 80 (2017) 046301. doi:10.1088/1361-6633/aa5bc5.
- [8] M. J. Dolinski, A. W. P. Poon, W. Rodejohann, Neutrinoless Double-Beta Decay: Status and Prospects, *Ann. Rev. Nucl. Part. Sci.* 69 (2019) 219. doi:10.1146/annurev-nucl-101918-023407.
- [9] H. Ejiri, J. Suhonen, K. Zuber, Neutrino–nuclear responses for astro-neutrinos, single beta decays and double beta decays, *Phys. Rept.* 797 (2019) 1. doi:10.1016/j.physrep.2018.12.001.
- [10] D. Q. Adams, et al., (CUORE Collaboration), High sensitivity neutrinoless double-beta decay search with one tonne-year of CUORE data (2021). arXiv:2104.06906v1.
- [11] M. Agostini, et al., (GERDA Collaboration), Final results of GERDA on the search for neutrinoless double- β decay, *Phys. Rev. Lett.* 125 (2020) 252502. doi:10.1103/PhysRevLett.125.252502.
- [12] G. Anton, et al., (EXO-200 Collaboration), Search for neutrinoless double- β decay with the complete EXO-200 dataset, *Phys. Rev. Lett.* 123 (2019) 161802. doi:10.1103/PhysRevLett.123.161802.
- [13] S. I. Alvis, et al., (MAJORANA Collaboration), Search for neutrinoless double- β decay in ^{76}Ge with 26 kg yr of exposure from the MAJORANA DEMONSTRATOR, *Phys. Rev. C* 100 (2019) 025501. doi:10.1103/PhysRevC.100.025501.
- [14] O. Azzolini, et al., (CUPID Collaboration), Final result of CUPID-0 Phase-I in the search for the ^{82}Se neutrinoless double- β decay, *Phys. Rev. Lett.* 123 (2019) 032501. doi:10.1103/PhysRevLett.123.032501.
- [15] R. Arnold, et al., (NEMO Collaboration), Measurement of the $2\nu\beta\beta$ decay half-life and search for the $0\nu\beta\beta$ decay of ^{116}Cd with the NEMO-3 detector, *Phys. Rev. D* 95 (2017) 012007.
- [16] A. Gando, et al., (KamLAND-Zen Collaboration), Search for majorana neutrinos near the inverted mass hierarchy region with KamLAND-Zen, *Phys. Rev. Lett.* 117 (2016) 082503. doi:10.1103/PhysRevLett.117.082503.
- [17] M. Agostini, A. M. Bakalyarov, M. Balata, I. Barabanov, L. Baudis, et al., Probing Majorana neutrinos with double- β decay, *Science* 365 (2019) 1445–1448. doi:10.1126/science.aav8613.
- [18] S. D. Biller, Combined constraints on Majorana masses from neutrinoless double beta decay experiments, *Phys. Rev. D* 104 (2021) 012002. doi:10.1103/PhysRevD.104.012002.
- [19] M. Agostini, G. Benato, J. A. Detwiler, J. Menéndez, F. Vissani, Testing the inverted neutrino mass ordering with neutrinoless double-beta decay (2021). arXiv:2107.09104v2.
- [20] J. Kotila, F. Iachello, Phase-space factors for double- β decay, *Phys. Rev. C* 85 (2012) 034316. doi:10.1103/PhysRevC.85.034316.
- [21] M. Wang, W. Huang, F. Kondev, G. Audi, S. Naimi, The AME 2020 atomic mass evaluation (II). tables, graphs and references, *Chinese Physics C* 45 (3) (2021) 030003. doi:10.1088/1674-1137/abddaf.
- [22] R. A. Damerow, R. R. Ries, W. H. Johnson, Atomic masses from ruthenium to xenon, *Phys. Rev.* 132 (1963) 1673–1681. doi:10.1103/PhysRev.132.1673.
- [23] T. Eronen, et al., JYFLTRAP: a Penning trap for precision mass spectroscopy and isobaric purification, *Eur. Phys. J. A* 48 (4) (2012) 46. doi:10.1140/epja/i2012-12046-1.
- [24] S. Eliseev, D. Nesterenko, K. Blaum, M. Block, C. Droese, F. Herfurth, E. Minaya Ramirez, Y. N. Novikov, L. Schweikhard, K. Zuber, q values for neutrinoless double-electron capture in ^{96}Ru , ^{162}Er , and ^{168}Yb , *Phys. Rev. C* 83 (2011) 038501. doi:10.1103/PhysRevC.83.038501.
- [25] J. Hyvärinen, J. Suhonen, Nuclear matrix elements for $0\nu\beta\beta$ decays with light or heavy Majorana-neutrino exchange, *Phys. Rev. C* 91 (2015) 024613. doi:10.1103/PhysRevC.91.024613.
- [26] F. Šimkovic, A. Faessler, V. Rodin, P. Vogel, J. Engel, Anatomy of the $0\nu\beta\beta$ nuclear matrix elements, *Phys. Rev. C* 77 (2008) 045503. doi:10.1103/PhysRevC.77.045503.
- [27] J. Barea, F. Iachello, Neutrinoless double-beta decay in the microscopic interacting boson model, *Phys. Rev. C* 79 (2009) 044301. doi:10.1103/PhysRevC.79.044301.
- [28] J. Barea, J. Kotila, F. Iachello, $0\nu\beta\beta$ and $2\nu\beta\beta$ nuclear matrix elements in the interacting boson model with isospin restoration, *Phys. Rev. C* 91 (3) (2015) 034304. arXiv:1506.08530, doi:10.1103/PhysRevC.91.034304.
- [29] J. T. Suhonen, Value of the axial-vector coupling strength in β and β decays: A review, *Front. Phys.* 5 (2017) 55.
- [30] I. Moore, et al., Towards commissioning the new IGISOL-4 facility, *Nucl. Instrum. Methods Phys. Res. B* 317 (2013) 208 – 213. doi:http://dx.doi.org/10.1016/j.nimb.2013.06.036.
- [31] S. Rahaman, V.-V. Elomaa, T. Eronen, J. Hakala, A. Jokinen, J. Julin, A. Kankainen, A. Saastamoinen, J. Suhonen, C. Weber, J. Äystö, Q values of the ^{76}Ge and ^{100}Mo double-beta decays, *Phys. Lett. B* 662 (2) (2008) 111 – 116. doi:10.1016/j.physletb.2008.02.047.
- [32] M. Vilén, et al., A new off-line ion source facility at IGISOL,

- Nucl. Instrum. Meth. Phys. Res. Sect. B (2019). doi:10.1016/j.nimb.2019.04.051.
- [33] A. Nieminen, J. Huikari, A. Jokinen, J. Äystö, P. Campbell, E. Cochrane, Beam cooler for low-energy radioactive ions, Nucl. Instrum. Meth. Phys. Res. A 469 (2) (2001) 244 – 253. doi:10.1016/S0168-9002(00)00750-6.
- [34] G. Savard, S. Becker, G. Bollen, H. J. Kluge, R. B. Moore, T. Otto, L. Schweikhard, H. Stolzenberg, U. Wiess, A new cooling technique for heavy ions in a Penning trap, Phys. Lett. A 158 (5) (1991) 247 – 252. doi:10.1016/0375-9601(91)91008-2.
- [35] S. Eliseev, K. Blaum, M. Block, C. Droese, M. Goncharov, E. Minaya Ramirez, D. A. Nesterenko, Y. N. Novikov, L. Schweikhard, Phase-imaging ion-cyclotron-resonance measurements for short-lived nuclides, Phys. Rev. Lett. 110 (2013) 082501. doi:10.1103/PhysRevLett.110.082501.
- [36] S. Eliseev, et al., A phase-imaging technique for cyclotron-frequency measurements, Applied Physics B 114 (1) (2014) 107–128. doi:10.1007/s00340-013-5621-0.
- [37] D. A. Nesterenko, et al., Phase-Imaging Ion-Cyclotron-Resonance technique at the JYFLTRAP double Penning trap mass spectrometer, Eur. Phys. J. A 54 (2018) 154. doi:10.1140/epja/i2018-12589-y.
- [38] D. Nesterenko, T. Eronen, Z. Ge, A. Kankainen, M. Vilen, Study of radial motion phase advance during motion excitations in a penning trap and accuracy of JYFLTRAP mass spectrometer, The European Physical Journal A 57 (2021) 302. doi:10.1140/epja/s10050-021-00608-3.
- [39] C. Roux, et al., Data analysis of Q -value measurements for double-electron capture with SHIPTRAP, The European Physical Journal D 67 (7) (2013) 146. doi:10.1140/epjd/e2013-40110-x.
- [40] A. Kellerbauer, K. Blaum, G. Bollen, F. H. H.-J. Kluge, M. Kuckein, E. Sauvan, C. Scheidenberger, L. Schweikhard, From direct to absolute mass measurements: A study of the accuracy of ISOLTRAP, Eur. Phys. J. D 22 (2003) 53–64. doi:10.1140/epjd/e2002-00222-0.
- [41] NIST, Atomic spectra database (2021). doi:10.18434/T4W30F. URL <https://www.nist.gov/pml/atomic-spectra-database>
- [42] W. Huang, M. Wang, F. Kondev, G. Audi, S. Naimi, The AME 2020 atomic mass evaluation (i). evaluation of input data, and adjustment procedures, Chinese Physics C 45 (3) (2021) 030002. doi:10.1088/1674-1137/abddb0.
- [43] M. Doi, T. Kotani, H. Nishiura, K. Okuda, E. Takasugi, Neutrino Mass, the Right-Handed Interaction and the Double Beta Decay. I: Formalism, Progress of Theoretical Physics 66 (5) (1981) 1739–1764. arXiv:<https://academic.oup.com/ptp/article-pdf/66/5/1739/5191494/66-5-1739.pdf>, doi:10.1143/PTP.66.1739. URL <https://doi.org/10.1143/PTP.66.1739>
- [44] M. Doi, T. Kotani, H. Nishiura, E. Takasugi, Double Beta Decay, Progress of Theoretical Physics 69 (2) (1983) 602–635. arXiv:<https://academic.oup.com/ptp/article-pdf/69/2/602/5252546/69-2-602.pdf>, doi:10.1143/PTP.69.602. URL <https://doi.org/10.1143/PTP.69.602>
- [45] H. Primakoff, S. P. Rosen, Double beta decay, Reports on Progress in Physics 22 (1) (1959) 121–166. doi:10.1088/0034-4885/22/1/305. URL <https://doi.org/10.1088/0034-4885/22/1/305>
- [46] T. Tomoda, Double beta decay, Reports on Progress in Physics 54 (1) (1991) 53–126. doi:10.1088/0034-4885/54/1/002. URL <https://doi.org/10.1088/0034-4885/54/1/002>
- [47] L. Jokiniemi, H. Ejiri, D. Frekers, J. Suhonen, Neutrinoless $\beta\beta$ nuclear matrix elements using isovector spin-dipole $J^\pi = 2^-$ data, Phys. Rev. C 98 (2018) 024608. doi:10.1103/PhysRevC.98.024608.
- [48] L. Jokiniemi, J. Suhonen, Muon-capture strength functions in intermediate nuclei of $0\nu\beta\beta$ decays, Phys. Rev. C 100 (2019) 014619. doi:10.1103/PhysRevC.100.014619.
- [49] A. Bohr, B. R. Mottelson, Nuclear Structure, Vol. I, Benjamin, New York, 1969.
- [50] K. Holinde, Two-nucleon forces and nuclear matter, Phys. Rep. 68 (1981) 121. doi:10.1016/0370-1573(81)90188-5.
- [51] J. Suhonen, O. Civitarese, Weak interaction and nuclear structure aspects of nuclear double beta decay, Phys. Rep. 300 (1998) 123.
- [52] F. Šimkovic, V. Rodin, A. Faessler, P. Vogel, $0\nu\beta\beta$ and $2\nu\beta\beta$ nuclear matrix elements, quasiparticle random-phase approximation, and isospin symmetry restoration, Phys. Rev. C 87 (2013) 045501. doi:10.1103/PhysRevC.87.045501.
- [53] J. Suhonen, From Nucleons to Nucleus: Concepts of Microscopic Nuclear Theory, Springer, Berlin, 2007.
- [54] A. Arima, T. Ohtsuka, F. Iachello, I. Talmi, Collective nuclear states as symmetric couplings of proton and neutron excitations, Phys. Lett. B 66 (3) (1977) 205 – 208. doi:[https://doi.org/10.1016/0370-2693\(77\)90860-7](https://doi.org/10.1016/0370-2693(77)90860-7). URL <http://www.sciencedirect.com/science/article/pii/S0370269377908607>
- [55] F. Iachello, A. Arima, The Interacting Boson Model, Cambridge University Press, 1987.
- [56] T. Otsuka, A. Arima, F. Iachello, Nuclear shell model and interacting bosons, Nucl. Phys. A 309 (1) (1978) 1 – 33. doi:[https://doi.org/10.1016/0375-9474\(78\)90532-8](https://doi.org/10.1016/0375-9474(78)90532-8). URL <http://www.sciencedirect.com/science/article/pii/S0375947478905328>
- [57] J. Kotila, J. Barea, Occupation probabilities of single particle levels using the microscopic interacting boson model: Application to some nuclei of interest in neutrinoless double- β decay, Phys. Rev. C 94 (2016) 034320. doi:10.1103/PhysRevC.94.034320. URL <https://link.aps.org/doi/10.1103/PhysRevC.94.034320>
- [58] J. Engel, Uncertainties in nuclear matrix elements for neutrinoless double-beta decay, Journal of Physics G: Nuclear and Particle Physics 42 (3) (2015) 034017. doi:10.1088/0954-3899/42/3/034017. URL <https://doi.org/10.1088/0954-3899/42/3/034017>
- [59] J. Barea, J. Kotila, F. Iachello, Nuclear matrix elements for double- β decay, Phys. Rev. C 87 (1) (2013) 014315. arXiv:1301.4203, doi:10.1103/PhysRevC.87.014315.
- [60] I. S. Towner, Phys. Rep. 155 (1987) 263–377. doi:10.1016/0370-1573(87)90138-4.
- [61] J. Suhonen, J. Kostensalo, Double β decay and the axial strength, Front. Phys. 7 (2019) 29.
- [62] F. Šimkovic, A. Faessler, H. Mütter, V. Rodin, M. Stauf, $0\nu\beta\beta$ -decay nuclear matrix elements with self-consistent short-range correlations, Phys. Rev. C 79 (2009) 055501. doi:10.1103/PhysRevC.79.055501.
- [63] R. Chandra, J. Singh, P. Rath, P. Raina, J. Hirsch, Two-neutrino double- β decay of $94 \leq a \leq 110$ nuclei for the $0^+ \rightarrow 0^+$ transition, Eur. Phys. J. A 23 (2005) 223. doi:10.1140/epja/i2004-10087-7.
- [64] A. Bobyk, W. Kamiński, P. Zareba, Study of the double beta decay of $70 \leq a \leq 100$ nuclei within the rqrpa and the self-consistent bcs + rqrpa formalisms, Nucl. Phys. A 669 (2000) 221. doi:10.1016/S0375-9474(99)00820-9.
- [65] P. K. Rath, R. Chandra, K. Chaturvedi, P. Lohani, P. K. Raina, J. G. Hirsch, Neutrinoless $\beta\beta$ decay transition matrix elements within mechanisms involving light majorana neutrinos, classical majorons, and sterile neutrinos, Phys. Rev. C 88 (2013) 064322. doi:10.1103/PhysRevC.88.064322.